Published in final edited form as:
Biochemistry. 2011 January 25; 50(3): 388–396. doi:10.1021/bi101239r.

The amino- and carboxyl-terminal fragments of the *Bacillus thuringensis* Cyt1Aa toxin have differential roles on toxin oligomerization and pore formation

Claudia Rodriguez-Almazan[1], **Iñigo Ruiz de Escudero**[2], **Pablo Emiliano Cantón**[1], **Carlos Muñoz-Garay**[1], **Claudia Pérez**[1], **Sarjeet S. Gill**[3], **Mario Soberón**[1], and **Alejandra Bravo**[1,*]

[1]Instituto de Biotecnología, Universidad Nacional Autónoma de México. Apdo. Postal 510-3, Cuernavaca 62250, Morelos (Mexico)

[2]Microbial Bioinsecticides, Instituto de Agrobiotecnología, CSIC-Universidad Publica de Navarra-Gobierno de Navarra, Mutilva Baja 31192, Spain

[3]Department of Cell Biology and Neuroscience, University of California, Riverside, CA 92506 (USA)

Abstract

The Cyt toxins produced by the bacteria *Bacillus thuringiensis* show insecticidal activity against some insects, mainly dipteran larvae, being able to kill mosquitoes and black flies. However, they also possess a general cytolytic activity *in vitro* showing hemolytic activity in red blood cells. These proteins are composed of two outer layers of α-helix hairpins wrapped around a β-sheet. Regarding to their mode of action, one model proposed that the two outer layers of α-helix hairpins swing away from the β-sheet allowing insertion of β-strands into the membrane forming a pore after toxin oligomerization. The other model suggested a detergent-like mechanism of action of the toxin on the surface of the lipid bilayer. In this work we cloned the N- and C-terminal domains form Cyt1Aa and analyzed their effects in Cyt1Aa toxin action. The N-terminal domain shows a dominant negative phenotype inhibiting the *in vitro* hemolytic activity of Cyt1Aa in red blood cells and the *in vivo* insecticidal activity of Cyt1Aa against *Aedes aegypti* larvae. In addition, N-terminal region is able to induce aggregation of Cyt1Aa toxin in solution. Finally, C-terminal domain composed mainly of β-strands, is able to bind to the SUV liposomes, suggesting that this region of the toxin is involved in membrane interaction. Overall, our data indicate that the two isolated domains of Cyt1Aa have different roles in toxin action. The N-terminal region is involved in toxin aggregation while the C-terminal domain in the interaction of the toxin with the lipid membrane.

Bacillus thuringiensis (Bt) spore-forming bacteria produce crystalline inclusions during their sporulation phase of growth. These inclusion bodies are composed of insecticidal proteins, also known as δ-endotoxins that comprise two multigenic families, named Cry and Cyt (1). Cry toxins have been found in many Bt strains and include proteins that are toxic to different insect orders such as Lepidoptera, Diptera, Coleoptera, or Hymenoptera and to nematodes (1). In contrast, the Cyt toxins show dipteran specificity *in vivo,* being able to kill mosquitoes and black flies (1). However, it is possible that Cyt proteins may have an even broader spectrum of activity against insects, since other specificities of Cyt toxins have been reported, i. e. Federici and Bauer (1998) showed that Cyt1Aa is toxic against a coleopteran larvae, the cottonwood leaf beetle (2). In addition to its *in vivo* insecticidal activity, the Cyt toxins showed *in vitro* cytolytic activity to a broad range of other cells, including

*Corresponding author: bravo@ibt.unam.mx phone 52 777 3291635, fax 52 777 3291624.

erythrocytes (1). Cyt toxins have been most frequently found in Bt strains active against mosquitoes in combination with Cry toxins that are also specific against dipteran larvae (1). It was shown that combination of dipteran specific Cry proteins with Cyt induces a synergistic activity among them. Due to this synergism their insecticidal activity is potentiated several fold above their combined individual toxicities (3–5), and that is why they have been used extensively for mosquito control. Several insecticidal products such as Vectobac, Teknar, Bactimos, Skeetal, and Mosquito Attack are now available for the control of mosquitoes such as *Aedes aegypti*, and certain *Anopheles* species vectors of dengue fever, and malaria, respectively, or against *Simulium damnosum* a black fly, vector of onchocearciasis (6–8).

Cry and Cyt are pore-forming toxins but they show different three-dimensional structures and mechanisms of action. Cyt proteins are composed of a single α–β domain comprising of two outer layers of α-helix hairpins wrapped around a β-sheet (9). The α–helices have an amphiphilic character, with the hydrophobic residues packed against the β-sheet. The α-helices are not long enough to span the membrane bilayer. In contrast, the β-strands 5 to 7 have an estimated length that could span the width of the biological membrane (9).

Cry and Cyt proteins are solubilized in the gut of susceptible dipteran insects and proteolytically activated by midgut proteases (8,10). Cry toxins show a complex mechanism of action involving multiple and sequential binding interactions with specific protein receptors located in the microvilli of midgut epithelial cells (11,12). In contrast, Cyt toxins do not bind to protein receptors and directly interact with non-saturated membrane lipids such as phosphatidylcholine, phosphatidylethanolamine and sphingomyelin (8,13). Cyt toxin bound irreversibly to the cell membrane inducing the formation of cation-selective channels in planar bilayers and release of radio-labeled solutes from the membrane vesicles (14,15).

There are currently two proposed models to explain the mechanism of action of Cyt toxins. One model proposed that the two outer layers of α-helix hairpins swing away from the β-sheet upon membrane contact and the long β-strands are allowed to insert into the membrane. Oligomerization proceeds ending with a formation of a structured β-barrel pore within the membrane, that kills the cells by colloid osmotic lysis (16). It was proposed that α–helix hairpin C–D is the hinge for the main conformational change; leaving the α–helices on the membrane surface and allowing that part of the β-sheet domain penetrate the hydrophobic zone of the bilayer (16). Studies performed with synthetic peptides of Cyt1A, showed that peptides corresponding to helices αA and αC are major structural elements involved in the membrane interaction and also affected the intermolecular assembly of the toxin since they were able to increase the insertion of the Cyt1Aa toxin into the membrane (17). Finally, the other model of the mechanism of action of Cyt toxins, proposed a nonspecific aggregation of the toxin on the surface of the lipid bilayer leading to a detergent action that leads to membrane disassembly and cell death (18).

Regarding to the molecular mechanism involved in the synergism between Cry and Cyt toxins, it was proposed that Cyt1Aa synergizes the toxic activity of Cry11Aa by functioning as a membrane-bound receptor (19). The specific epitopes involved in their interaction have been mapped in both toxins, and mutations in these residues severely affected their synergism (19). Additionally, it was shown that the binding of Cry11Aa to Cyt1Aa toxin facilitates the formation of a Cry11Aa oligomeric structure that is capable of forming pores in membrane vesicles (20).

Recently, it was shown that Cyt2Ba toxin share partial sequence similarity and a similar topological organization with the volvatoxin A2 (VVA2), a pore forming cardiotoxin from mushroom *Volvariella volvacea* (21). Interestingly, the VVA2 is also hemolytic against red

blood cells and a functional study performed with isolated domains of the VVA2 showed that N-terminal domain, that comprised the region rich in α-helices, is responsible of oligomerization of VVA2 toxin in absence of membrane lipids and inhibited the hemolytic activity of the toxin acting as a dominant negative inhibitor (22). In contrast, the C- terminal domain, harboring the three long β-strands is involved in binding and insertion into the membrane (22).

In this work we cloned the N- and C-terminal fragments of Cyt1Aa toxin, and analyzed their functional role. We found that similar to the VVA2 toxin, the N-terminal region of Cyt1Aa induced toxin aggregation in the absence of lipids and that this fragment has a dominant negative inhibitory effect on the hemolytic activity of Cyt1Aa. We also found that N-terminal region inhibits the *in vivo* insecticidal activity against *Aedes aegypti* larvae. Finally, our data confirmed that C-terminal domain of Cyt1Aa, a region that is rich in β-strands, is involved in membrane interaction.

EXPERIMENTAL PROCEDURES

Cloning and expression of N-terminal and C-terminal fragments of Cyt1Aa

We first cloned p20 protein gene that codifies for a chaperon protein necessary for the correct folding of the Cyt1Aa protein (23) into pHT315 plasmid (24) and then we used this construction named pHT315-p20 to clone the *cyt*1Aa gene or the two Cyt1Aa fragments. The p20 gene was amplified using total Bti DNA as template using p20f forward and p20r reverse primers (Table 1) that contain a *Xma*I restriction site in their 5' end. This PCR product was cloned into the unique *Xma*I site of the pHT315 plasmid to construct pHT315-p20.

The *cyt*1A gene was amplified using plasmid pWF45 (25) as template and Vent-Polymerase (New England BioLabs, Beverly, MA). The primers used for this reaction, pCytf forward and pCytr reverse primers (Table 1) include a *HindIII* and *KpnI* restriction sites at their 5' end, respectively. This PCR product was cloned into pHT315-p20 vector previously digested with *HindIII* and *KpnI* restriction enzymes and transformed into *B. thuringiensis* 407 acrystalliferous strain (24). This construction was named pHT315-cyt1Aa.

Two PCR reactions were performed with plasmid pWF45 as template for construction of each N-terminal or C-terminal fragments. The first PCR reaction for N-terminal fragment amplifies 834 bp that includes the promotor region of *cyt*1Aa gene and the first 170 residues of the toxin (Fig. 1A). This PCR reaction was performed with pCytf forward primer and pNT1r reverse primer that includes nine nucleotides (underlined) at 5' end which corresponds to a stop codon (in bold) and the beginning of the terminator region of the gene (Table 1). The second PCR reaction for N-terminal fragment amplifies 348 bp corresponding to the terminator region. For this PCR reaction we used pNT2f forward primer that completely overlaps with PNT1r and pCytr reverse primers (Fig. 1A, Table 1). The PCR products were purified with the QIAquick PCR Purification Kit (QIAGEN, Valencia, CA) and used as megaprimers in a second PCR reaction of eight cycles performed with Vent-Polymerase. Finally, pCytf and pCytr primers were added to the reaction mixture and amplification was continued for other 30 cycles (Fig 1A). The expected PCR product of the complete N-terminal domain was 1149 bp.

In the case of amplification of C-terminal fragment, the first PCR reaction amplifies 346 bp that includes the promotor region of *cyt*1Aa gene and 21 nucleotides from C-terminal region starting in residue 168. This PCR reaction was performed with pCytf forward primer and pCT1r reverse primer that includes the 21 nucleotides (underlined) mentioned above (Table 1, Fig. 1A). The second PCR reaction for C-terminal fragment amplifies 585 bp

corresponding to the last 80 residues of Cyt1Aa (from residue 168 to 248) and the terminator region. For this reaction we used pCT2 forward primer that overlaps completely with pCT1r and pCytr reverse primer (Table 1, Fig. 1A). These two PCR products were purified with QIAquick PCR Purification Kit and used as megaprimers in a PCR reaction as described above for N-terminal fragment amplification. After eight cycles of amplification primers pCytf and pCytr were added and reaction continued for 30 cycles. The expected PCR product of the complete C-terminal domain was 898 bp. The final PCR fragments were purified with QIAquick PCR Purification Kit, and ligated blunt into pJET plasmid.

Both DNA constructions were first electroporated into *E. coli* DH5α cells. Plasmids were purified and digested with *HindIII* and *XbaI* (New England BioLabs, Beverly, MA). The *HindIII* site was included in the PCR products and the *XbaI* restriction site is present in the pJET plasmid. Finally the purified digested fragments were ligated into vector pHT315-p20 previously digested with same restriction enzymes and transformed into *B. thuringiensis* 407 acrystalliferous strain (24). These constructions were named pHT315-CytNter and pHT315-CytCter, respectively.

Purification of Cyt1Aa protein, N-terminal or C-terminal domains

Bt bacterial strains containing pHT315-Cyt1Aa, pHT315-CytNter or pHT315-CytCter plasmids were grown at 200 rpm and 30°C in HCT sporulation medium (26) supplemented with 10 μg/ml erythromycin. Spores and crystal inclusions produced by the Bt strains were harvested and washed three times with 0.3 M NaCl, 0.01 M EDTA, pH 8.0. The pellet was suspended in 0.05% Triton X-100, 300 mM NaCl, 20 mM Tris-HCl pH 7.2, sonicated two times 1 min and inclusions were purified by sucrose gradient centrifugation (27). This procedure was performed twice. Protein concentration was determined by the Bradford assay. Purified Cyt1Aa, N-terminal and C-terminal fragment crystals were visualized in von Jagow SDS-PAGE acrilamide gradient (4 to 16 %) SDS-PAGE gels (28) stained with silver or visualized by Western blot as described below. Finally, these proteins were solubilized in 50 mM Na_2CO_3, 1 mM DTT, pH 10.5. Cyt1Aa protoxin was activated with 1:30 proteinase K (Sigma-Aldrich Co.) w/w for 1 h at 30°C.

Western Blot

Protein samples were boiled for 5 min in Laemmli sample loading buffer, separated in SDS-PAGE and electrotransferred onto PVDF membrane (Millipore, Bedford, MA). The Cyt1Aa protein or their corresponding N- or C-terminal domains were detected using anti-Cyt1Aa1/11 polyclonal antibody (1/30000, 1h) that was raised in rabbits against Cyt1Aa toxin and a secondary antibody coupled with horseradish peroxidase (HRP) (Sigma, St Louis, MO) (1/5000, 1h) followed by luminol (ECL; Amersham Pharmacia Biotech) as described by the manufacturers. Molecular weight markers used in all SDS-PAGE were precision pre-stained plus standards, all blue (BioRad).

Hemolysis assay

Hemolytic assays were done as previously described (29). Shortly, human red blood cells were diluted to a concentration of 2×10^8 cells /ml in buffer A (0.1 M dextrose ; 0.07 M NaCl, 0.02 M sodium citrate, 0.002 M citrate, pH 7.4). The final volume of reaction mixture was 0.2 ml containing 20 μl of washed blood cells and various concentrations of Cyt1Aa in the same buffer were incubated at 37°C for 30 min in a 96 well tissue culture plates. The supernatants were collected by centrifugation at 1,290 *xg* for 5 min at 4°C and hemolytic activity was quantitated measuring the absorbance of the supernatant at 405 nm. 100% hemolysis was defined as the same volume of human red blood cell solution incubated with dechlorinated H_2O. For analysis of inhibition of the hemolytic activity of Cyt1Aa in the presence of N-terminal or C-terminal fragments, we used mixtures with different ratios as

stated in the text. The concentration of Cyt1Aa used in these hemolysis inhibition experiments was 60 ng/ml, which induced 80 % hemolytic activity. These assays were done four times. A *t*-test made with the statistical program GraphPad Prism was used to analyze differences between observed mean values of percentage of hemolysis induced by the toxin:fragment mixtures compared with the control (Cyt1Aa:fragment 1:0 ratio). P value <0.01, 95% confidence interval were considered statistical significant. Bars labeled with different letters indicated that differences were statistically significant.

Insect bioassay

Mosquitocidal bioassays were performed against 20 early 4th-instar larvae in 100 ml of dechlorinated water. Ten different concentrations of purified Cyt1Aa crystals were used (50 to 6000 ng/ml). Positive (Bti) and negative controls (dechlorinated water) were included in the bioassay, and larvae viability examined 24 h after treatment. The mean lethal concentration (LC_{50}) was estimated by Probit analysis using statistical parameters (30) after four independent assays (Polo-PC LeOra Software). For inhibition studies we use a Cyt1Aa toxin concentration that kill 85% of the larvae (1.2 μg/ml) mixed with N-terminal or C-terminal domains at different protein ratios of Cyt1Aa: N- or C-terminal domain (1:1, 1:0.5 and 1:0.1). A *t*-test was used to analyze differences between observed mean values of percentage of mortality induced by the toxin:fragment mixtures compared with the control (Cyt1Aa:fragment 1:0 ratio). Bars labeled with different letters indicated that differences were statistically significant.

Preparation of Small Unilamellar Vesicles (SUV)

Egg-yolk phosphatidyl choline (PC), cholesterol (Ch) (Avanti Polar Lipids, Alabaster, AL) and stearylamine (S) (Sigma St Louis, MO) from a chloroform stocks, were mixed in glass vials in a 10:3:1 proportion, respectively, at 2.6 μmol final concentration of the total lipid mixture and dried by argon flow evaporation followed by overnight storage under vacuum to remove residual chloroform. The lipids were hydrated in 2.6 ml of 10 mM CHES, 150 mM KCl pH 9 by a 30 min incubation followed by vortex. To prepare SUV the lipid suspension was subjected to sonication two times for two min in a Branson-1200 bath sonicator (Danbury, CT). SUV were used within 2–3 days upon their preparation.

Oligomerization of Cyt1Aa toxin

The oligomerization of Cyt1Aa was induced by incubation of 2 μg of Cyt1Aa solubilized protoxin with 0.03 μmol SUV liposomes and 0.01 μg of proteinase K during 20 min at 30°C. 1mM final concentration of PMSF was added to stop the reaction. Samples were boiled 2 min, loaded in SDS-PAGE von Jagow gradient gels and developed by Western blot as described above. Analysis of aggregation of Cyt1Aa was also done in solution in the absence of liposomes and in presence of different ratios of N- or C-terminal fragments as described in the text.

Binding assays and binding competition

The binding interaction of N-or C-terminal fragments to the SUV liposomes (0.03 μmol) was analyzed in 50 μl binding buffer (PBS, 0.1% BSA w/v, 0.05% Tween 20 v/v, pH 7.6). After 1h incubation at 25 °C the membrane pellets were centrifuged at 90,000 rpm for 30 min. The resulting membrane pellets or supernatants were boiled 5 min in Laemmli sample loading buffer, loaded in SDS-PAGE and transferred to Hybond-ECL nitrocellulose membranes (Amersham Biosciences). The presence of C- or N-terminal fragments in the pellet or in the supernatants was then analyzed by Western blot.

.

For binding competition assays the SUV liposomes (0.03 μmol) were incubated in 50 μl binding buffer with 2 nM biotinylated wild type Cyt1Aa toxin (RPN28, Amersham Biosciences) in the absence or presence of different fold excesses (100 or 1000) of unlabeled N- or C- terminal fragments for 1h. Unbound toxin was washed twice by centrifugation (30 min at 90,000 ×*g*). The resulting membrane pellet was boiled, loaded in SDS-PAGE and transferred to nitrocellulose membranes as described above. The biotinylated toxin bound to the liposomes, was visualized by incubating with streptavidin-HRP conjugate (1:4000 dilution) for 1 h, and developed with luminol as described by the manufacturers. Scanning of the 25 kDa signal was performed to quantify binding.

Fluorescence Measurements

Calcein leakage experiments were performed as described (31). Calcein containing vesicles were prepared by sonication (two times for two min) of the SUV in calcein 80 mM (Molecular probes, Eugene Oregon) dissolved in 150 mM KCl, 10 mM CHES, pH 9. Non-entrapped calcein was removed by gel filtration on Sephadex G-50 (1 cm × 30 cm column) eluted with the same buffer. Calcein loaded SUV, 100 μl, were added to 900 μl 150 mM KCl, CHES 10 mM, pH 9. Finally, samples of Cyt1Aa toxin or each of the Cyt1Aa-domains were added and the release of calcein was analyzed during time. The calcein is released because the SUV were disrupted due to interaction of the toxin with the membrane and then the released calcein showed an increase in fluorescence due to the dequenching of the dye into the external medium. Calcein fluorescence was excited at 490 nm (10 nm slit) and monitored at 520 nm with an Aminco Bowman Luminescence Spectrometer (Urbana IL, USA). Maximal leakage at the end of each experiment was assessed by lysis with 0.1% Triton-X-100 (final concentration). All fluorescence experiments were performed in triplicate at 25 °C. A *t*-test was used to analyze differences between observed mean values of percentage of calcein released by different concentrations of Cyt1Aa or the toxin fragments when compared with the control (No-toxin). Bars labeled with different letters indicated that differences were statistically significant.

RESULTS

Role of N- and C-terminal fragments on Cyt1Aa toxin activity

The N- and C-terminal fragments of Cyt1Aa were cloned separately into pHT315 and these new constructions were named pHT315-CytNter and pHT315-CytCter, respectively. Both of these protein fragments were expressed separately in *B. thurngiensis* Bt 407 strain and crystal inclusions were purified. Figure 1A shows the schematic diagram of PCR amplification strategy of the two fragments and figure 1B shows the putative three-dimensional structure of the two Cyt1Aa fragments according to the described coordinates of Cyt2Aa. The N terminal fragment produces a protein of 18.9 kDa, and the C terminal fragment a protein of 8.8 kDa. Figure 1C shows a silver stained von Jagow SDS-PAGE gradient gel and figure 1D the Western blot detection of the two Cyt1Aa fragments produced in Bt cells.

The hemolytic activity of activated Cyt1Aa against red blood cells was analyzed showing a medium effective concentration (EC_{50}) value of 48 ng/ml (Fig. 2A). The two Cyt1Aa fragments or the p20 protein were inactive and the mixture of N- and C-terminal fragments was also unable to induce hemolysis.

We then analyzed the effect of N- and C- terminal fragments on Cyt1Aa hemolytic activity. Different molar ratios of the N- and C- terminal fragments were pre-mixed with a Cyt1Aa protein concentration that gave 80 % hemolytic activity (60 ng/ml) as indicated in figure 2B and the percentage of hemolytic activity of Cyt1Aa was determined. Each value represents

the mean ±SD after four independent experiments. The N-terminal fragment inhibited >93% of Cyt1Aa hemolysis at 1:0.5 or 1:1 ratios. In contrast, the C-terminal fragment showed a much lower inhibition of Cyt1Aa hemolysis since at 1:0.5 ratio the inhibition of hemolysis of Cyt1Aa was not statistically significant with a P value of 0.1002. At 1:1 ratio the C-terminal inhibited only 27% of total hemolytic activity (P value 0.0009) and only at 1:10 ratio we observed a clear 75% inhibition of total Cyt1Aa hemolytic activity (P value 0.0001). Finally, the control performed with p20 protein at 1:10 ratio did not affected the hemolytic activity of Cyt1Aa (Fig 2B).

The toxicity of Cyt1Aa protoxin was also analyzed in bioassays by feeding fourth instar *A. aegypti* larvae with Cyt1Aa crystal suspension. The medium lethal concentration showed a value of 660 ng/ml (463–929, 95% confidential limits). In contrast the N- and C-terminal fragments and the p20 protein were completely inactive when tested individually in bioassays against *A. aegypti* at 10 μg/ml. We then analyzed the effect of these fragments on Cyt1Aa toxicity, using a toxin concentration that kills 80 % of the larvae (1.2 μg/ml) mixed with different molar ratios of purified crystals from the N- or C-terminal fragments. The N-terminal fragment was highly effective to block insecticidal activity since at 1:0.5 or 1:1 ratios were able to inhibit > 70 % of the insecticidal activity of Cyt1Aa toxin *in vivo* (P value 0.0001). In contrast to the C-terminal fragment or the p20 protein that did not inhibit the toxicity of Cyt1Aa toxin even at 1:10 ratio (Fig. 2C) with a P value of 1 indicating that differences in these assays were not statistically significant.

Oligomerization of Cyt1A

It was previously shown that Cyt1Aa protein was able to from large aggregates that migrated as a high molecular size band in a SDS-PAGE after interaction with liposomes or with different cells (32). The aggregate shows to be highly stable under the denaturant conditions of SDS-PAGE gels where the sample is boiled and was also analyzed in gradient centrifugation (32). We analyzed the aggregation of Cyt1Aa toxin after interaction with of SUV liposomes prepared with a mixture of 10:3:1 of phosphatidyl choline (PC), cholesterol (Ch) and stearylamine (S) as described in experimental procedures. We incubated Cyt1Aa protoxin in the presence of SUV liposomes and proteinase K and observed the formation of a similar high molecular size aggregate as previously described (32). This aggregate was also similar to the high molecular size aggregate observed when VVA2 toxin interacts with lipid membranes (22) (Fig. 3A). The observed band at the high molecular size shows a diffuse pattern, this could be due to a heterogeneous aggregate of monomers or aggregates may have a more hydrophobic structure as has been observed for the 250 kDa oligomers of Cry toxins (12). It is however quite important to note that in the absence of SUV the Cyt1Aa toxin was unable to form any kind of aggregate structure and remains as a monomeric structure (Fig 3A).

The aggregation of Cyt1Aa was then analyzed in the absence of SUV liposomes when different ratios of N- or C-terminal fragments were present in the assay. The N-terminal fragment induced the formation of a high molecular band similar to the one that was observed in presence of lipid membranes described above, suggesting that this fragment induced aggregation of Cyt1Aa in solution. The aggregation of Cyt1Aa was observed at very low concentration of N-terminal fragment (1:0.1 ratio, Cyt1Aa: N-terminal fragment) (Fig. 3B). In contrast the C-terminal fragment did not induce aggregation of Cyt1Aa in solution in the absence of SUV, even at a high concentration (1:10 ratio).

Interaction of N- and C-terminal fragments with the membrane

The binding interaction of N- or C-terminal fragments to the membrane was analyzed after 1h incubation with SUV. Figure 4A shows that C-terminal fragment was associated with the

membrane pellet. In contrast N-terminal fragment did not associate with the membrane and remained in solution (Fig. 4B).

It was previously reported that monoclonal antibody 10B9 that recognized the native form of the Cyt1Aa toxin inhibit 92% of the binding of the toxin to Cf1 cells from *Choristoneura fumiferana*, when used at 3:1 molar ratio (10B9:Cyt1Aa) (32). We analyzed if the interaction of C-terminal with the SUV liposomes domain could be also blocked by 10B9 antibody. Figure 4C shows that 10B9 antibody inhibited the toxin binding to the membrane pellet, suggesting that this C-terminal toxin fragment is interacting with the membrane in a similar way as the complete Cyt1Aa protein. In addition we performed binding competition assays analyzing the binding of biotin-labeled Cyt1Aa toxin to SUV liposomes in the presence of 100 fold or 1000 fold molar excess of C- or N- terminal fragments. Figure 4D shows that only C-terminal fragment was able to affect the interaction of the toxin with the SUV liposomes. All these data support the hypotheses that C-terminal region has a role in membrane interaction.

Finally, in order to confirm that C-terminal fragment was able to interact with the membrane, we analyzed if this protein fragment was able to form pores or affect the integrity of membrane liposomes. The integrity of lipid membrane vesicles was analyzed using calcein-release assays. The release of entrapped calcein from SUV was measured as dequenching of the calcein fluorescence, and was thereby monitored continuously as an increase in the fluorescence intensity. Data are expressed as percentage of the maximal fluorescence release, obtained with the positive control Triton X-100. The insert in figure 5 shows a representative trace showing that the Cyt1Aa induces a fast release of encapsulated calcein. A similar fast release of calcein was induced with soluble C-terminal fragment at 200 nM with a P value of 0.5992 that indicated that differences were not statistically significant from the result obtained with wild type toxin at the same concentration. In contrast, the N-terminal fragment was unable to affect the membrane integrity and did not release the entrapped calcein fluorophore. Calcein release is an indirect assay, and these data clearly indicated that C-terminal fragment is able to affect the integrity of the SUV liposomes. However, the exact mechanism of C-terminal action in the membrane still remains to be determined.

DISCUSSION

In this work we demonstrated that the two domains of Cyt1Aa may play a different role in toxin action. Our data suggest that the N-terminal region is important to induce toxin aggregation, while C-terminal domain is important for membrane binding and affects membrane permeability. Similar roles were previously described for the N- and C-terminal domains of VVA2 that shares a similar topological structure with Cyt1Aa. Overall our data suggest that both toxins, VVA2 and Cyt1Aa, may work with a similar mechanism of action. However it is very important to notice that they are different toxins that have different specificity of action *in vivo,* since Cyt1Aa is active against dipteran larvae in contrast to VVA2 that is a cardiotoxin that causes cardiac arrest by affecting Ca^{2+} accumulation in the microsomal fraction of the sarcoplasmic reticulum of the ventricular muscle in mammals. The main difference between these two proteins is that VVA2 toxin harbors a specificity domain composed of two extra β-strands that are absent in the Cyt1Aa protein. This region is involved in heparin binding on the cell membrane and is conserved among several cardiotoxins isolated from snake venoms. In contrast, the specificity domain of Cyt1Aa has not been clearly identified. However, Cyt1Aa is currently used worldwide in the control of mosquitoes then it is quite important to fully understand its mechanism of action.

The Cyt1Aa has high affinity for the lipids found in mosquito membranes, and it was reported previously that the interaction with lipids rapidly induces toxin aggregation. Large aggregates were observed after incubation of Cyt1Aa toxin with synthetic membranes such as PC (33) or mixtures of lipids such as PC:Ch:S (34). The association of Cyt toxins with membrane has also been analyzed after interaction with different cells (32). In the case of Cyt1Aa, it was previously shown that this protein is able to interact with Cf1 cells that is a cell line derived from *Ch. fumiferana* larvae or with human red blood cells inducing oligomerization (32). The molecular size of the oligomer was estimated in linear sucrose density gradients after incubation of iodinated toxin with these cells. The oligomer of Cyt1Aa in Cf1 showed a size of 400 kDa while in red blood cells was 170 kDa. The molecular size of aggregates remains constant even if higher toxin concentrations were used in the assay, suggesting an ordered oligomerization state of the toxin in each type of cells. Based in density gradient centrifugation analysis it was proposed that Cyt1Aa form high molecular weigh oligomers in insect cells composed of 16 monomer molecules (32). In other report, the association of Cyt2Aa with red blood cell was studied at different temperatures, showing that rate of pore formation was low at low temperatures suggesting that low temperature did not inhibit binding of the toxin to the membrane but markedly reduced oligomerization. It was proposed that Cyt2Aa toxin inserts into the membrane before oligomerization and then oligomerization of the toxin results in pore formation (35).

In this work, we show that Cyt1Aa toxin is able to form high molecular weight structures after incubation with the SUV liposomes composed of PC:Ch:S. In contrast, in solution the toxin remains in its monomer state. We found that N-terminal fragment was able to trigger aggregation of the toxin in solution forming aggregates with similar size as those found when the Cyt1Aa interacts with membrane lipids. The N-terminal fragment was also able to completely inhibit the hemolytic activity of the toxin *in vitro* and the *in vivo* insecticidal activity in mosquito larvae, showing a dominant negative phenotype. These results may suggest that the aggregate formed in the presence of the N-terminal fragment is inactive. However, this remains to be demonstrated. Recently it was reported that A61C and S108C mutants isolated in the closely related Cyt2Aa toxin, located in helices α-A and α-C respectively, did not form oligomeric structures after incubation with membrane liposomes. These mutants were severely affected in their hemolytic activity (36), supporting the hypothesis that these regions of Cyt toxins may have an important role in toxin action and that toxin oligomerization is a necessary step for toxin action. In another report, the authors analyzed the interaction of Cyt1Aa labeled with a fluorescent dye with PC liposomes. They reported that labeled-Cyt1Aa increased its interaction with the membrane if unlabelled toxin was added to the assay, suggesting that oligomerization of several monomers of the toxin increased its capacity to interact with the membrane. They also showed that unlabelled synthetic peptides corresponding to helices αA and αC increased the interaction of labeled-Cyt1Aa with the liposomes, suggesting that these regions of the toxin may serve as the structural seeding elements that trigger the oligomerization process of Cyt1Aa (17).

Our results also showed that the C-terminal domain is involved in interaction and insertion into the membrane. These data correlated with a previous study that showed that C-terminal region of the toxin was inserted into the membrane whereas the N-terminal region of the toxin could be removed when membrane bound-Cyt1Aa toxin was treated with proteases (34). In addition, fluorescence spectroscopy analysis of selected mutant proteins of Cyt1Aa, that were labeled with the polarity sensitive dye acrylodan, showed that strands β–5, β–6 and β–7 insert into the membrane (16). The authors suggested that the pores formed by Cyt1Aa toxin are assembled from the three major β-strands present in the C-terminal half of the toxin (16).

Finally, different data support that a structured pore inserted into the membrane is involved in the mechanism of action of Cyt1Aa. In the first place the Cyt1Aa forms ion channels when analyzed in planar lipid bilayers (14) and these data were supported by studies of the dissipation of diffusion potential as a measurement of toxin pore formation activity (17). The Cyt1Aa was more potent in permeating large unilamellar vesicles than SUV, indicating that the toxin form pores in the membrane rather than acting as a detergent (17). In this work, we reported that isolated C-terminal fragment was capable of inducing calcein release *in vitro* while it lacked biological activity. These observations could suggest that the function of N-terminal domain in triggering oligomerization of Cyt1Aa is required for *in vivo* toxicity against mosquito larvae and that the *in vitro* pore formation activity of the C-terminal fragment may result from a non-specific destruction of the membrane integrity that remains to be analyzed. It is also possible that C-terminal fragment may be degraded in the highly proteolytical environment of the midgut lumen of the larvae, explaining its lack of activity *in vivo*.

In summary, the results presented here allowed us to propose that Cyt1Aa toxin first bind the membrane as a monomer with some regions present in the C-terminal domain, then a conformational change induced in N-terminal domain triggers oligomerization of the toxin that leads to penetration of the β-strand present in the C-terminal domain into the lipid bilayer resulting in membrane permeabilization.

Acknowledgments

We thank Lizbeth Cabrera and Jorge Arturo Yañez for technical assistance.

Financial support: Research was funded in part through grants from the National Institutes of Health, 1R01 AI066014, DGAPA/UNAM IN218608 and IN210208-N, CONACyT U48631-Q 478. IRdE received a José Castillejo postdoctoral grant, and a mobility grant for teaching and research staff of UPNA, Spain.

Abbreviations

Cyt	cytolytic δ-endotoxin from *Bacillus thuringiensis*
Cry	crystal δ-endotoxin from *Bacillus thuringiensis*
Bt	*Bacillus thuringiensis*
Bti	*Bacillus thuringiensis* subsp *israelensis*
VVA2	cardiotoxin from *Volvariella volvacea*
SUV	small unilamellar vesicles
PC	phosphatidyl choline
Ch	cholesterol
S	stearylamine
EC_{50}	mean effective concentration
LC_{50}	mean lethal concentration

REFERENCES

1. de Maagd RA, Bravo A, Berry C, Crickmore N, Schnepf HE. Structure, diversity and evolution of protein toxins from spore-forming entomopathogenic bacteria. Ann. Rev. Genet. 2003; 37:409–433. [PubMed: 14616068]

2. Federici B, Bauer LS. Cyt1Aa protein of *Bacillus thuringiensis* is toxic to the cottonwood leaf beetle, *Chrysomela scripta*, and suppresses high levels of resistance to Cry3Aa. Appl. Environ. Microbiol. 1998; 64:4368–4371. [PubMed: 9797292]

3. Chilcott CN, Ellar DJ. Comparative study of *Bacillus thuringiensis* var. *israelensis* crystal proteins *in vivo* and *in vitro*. J. Gen. Microbiol. 1988; 134:2551–2558. [PubMed: 3254944]

4. Tabashnik B. Evaluation of synergism among *Bacillus thuringiensis* toxins. Appl. Environ. Microbiol. 1992; 58:3343–3346. [PubMed: 1444368]

5. Wu D, Johnson JJ, Frederici BA. Synergism of mosquitocidal toxicity between CytA and CryIVD proteins using inclusions produced from cloned genes of *Bacillus thuringiensis*. Mol. Microbiol. 1994; 13:965–972. [PubMed: 7854129]

6. Guillet, P.; Kurstak, DC.; Philippon, B.; Meyer, R. Use of *Bacillus thuringiensis israelensis* for Onchocerciasis control in West Africa. In: de Barjac, H.; Sutherland, DJ., editors. Bacterial control of mosquitoes and black flies. New Jersey: Rutgers University Press; 1990. p. 187

7. Becker, N. Bacterial control of vector-mosquitoes and black flies. In: Charles, JF.; Delécluse, A.; Nielsen-LeRoux, C., editors. Entomopathogenic bacteria, from laboratory to field application. Netherlands: Kluwer Academic Publishers; 2000. p. 383-396.

8. Bravo A, Gill SS, Soberón M. *Bacillus thuringiensis* mechanisms and use. Comprehensive Molecular Insect Science Elsevier BV. 2005:175–206.

9. Li J, Koni PA, Ellar DJ. Structure of the mosquitocidal delta-endotoxin CytB from *Bacillus thuringiensis* sp *kyushuensis* and implications for membrane pore formation. J. Mol. Biol. 1996; 257:129–152. [PubMed: 8632451]

10. Schnepf E, Crickmore N, Van Rie J, Lereclus D, Baum J, Feitelson J, Zeigler DR, Dean DH. *Bacillus thuringiensis* and its pesticidal crystal proteins. Microbiol. Mol. Biol. Rev. 1998; 62:775–806. [PubMed: 9729609]

11. Pacheco S, Gómez I, Arenas I, Saab-Rincon G, Rodríguez-Almazán C, Gill SS, Bravo A, Soberón M. Domain II loop 3 of *Bacillus thuringiensis* Cry1Ab toxin is involved in a “ping pong” binding mechanism with *Manduca sexta* aminopetidase-N and cadherin receptors. J. Biol. Chem. 2009; 284:32750–32757. [PubMed: 19808680]

12. Bravo A, Gómez I, Conde J, Muñoz-Garay C, Sánchez J, Miranda R, Zhuang M, Gill SS, Soberón M. Oligomerization triggers binding of a *Bacillus thuringiensis* Cry1Ab pore-forming toxin to aminopeptidase N receptor leading to insertion into membrane microdomains. Biochim. Biophys. Acta. 2004; 1667:38–46. [PubMed: 15533304]

13. Thomas WE, Ellar DJ. Mechanism of action of *Bacillus thuringiensis* var *israelensis* insecticidal δ-endotoxin. FEBS Lett. 1983; 154:362–368. [PubMed: 6832375]

14. Knowles BH, Blatt MR, Tester M, Horsnell JM, Carroll J, Menestrina G, Ellar DJ. A cytolytic δ-endotoxin from *Bacillus thuringiensis* forms cation-selective channels in planar lipid bilayers. FEBS Lett. 1989; 244:259–262. [PubMed: 2465921]

15. Knowles BH, White PJ, Nicholls CN, Ellar DJ. A broad-spectrum cytolytic toxin from *Bacillus thuringiensis* var. *kyushuensis*. Proc. Roy. Soc. ser. B. 1992; 248:1–7.

16. Promdonkoy B, Ellar DJ. membrane pore architecture of a cytolytic toxin from *Bacillus thuringiensis*. Biochem. J. 2000; 350:275–282. [PubMed: 10926854]

17. Gazit E, Burshtein N, Ellar DJ, Sawter T, Shai Y. *Bacillus thuringiensis* cytolytic toxin associates specifically with its synthetic helices A and C in the membrane bound state. Implications for assembly of oligomeric transmembrane pores. Biochemistry. 1997; 36:15546–15554. [PubMed: 9398283]

18. Butko P. Cytolytic toxin Cty1Aa and its mechanism of membrane damage: data and hypotheses. Appl. Environ. Microbiol. 2003; 69:2415–2422. [PubMed: 12732506]

19. Pérez C, Fernandez LE, Sun J, Folch JL, Gill SS, Soberón M, Bravo A. *Bti* Cry11Aa and Cyt1Aa toxins interactions support the synergism-model that Cyt1Aa functions as membrane-bound receptor. Proc. Nat. Acad. Sci. USA. 2005; 102:18303–18308. [PubMed: 16339907]

20. Pérez C, Muñoz-Garay C, Portugal LC, Sánchez J, Gill SS, Soberón M, Bravo A. *Bacillus thuringiensis* subsp. *israelensis* Cyt1Aa enhances activity of Cry11Aa toxin by facilitating the formation of a pre-pore oligomeric structure. Cell. Microbiol. 2007; 9:2931–2937. [PubMed: 17672866]

21. Cohen S, Dym O, Albeck S, Ben-Dov E, Cahan R, Firer M, Zaritsky A. High resolution crystal of activated Cyt2Ba monomer from *Bacillus thuringiensis* subs *israelensis*. J. Mol. Biol. 2008; 380:820–827. [PubMed: 18571667]
22. Weng Y-P, Lin Y-P, Hsu Ch-I, Lin J-Y. Functional domains of a pore-forming cardiotoxic protein Volvatoxin A2. J. Biol. Chem. 2004; 279:6805–6814. [PubMed: 14645370]
23. Wu D, Federeci BA. A 20-kilodalton protein preserves cell viability and promotes CytA crystal formation during sporulation in *Bacillus thuringiensis*. J. Bacteriol. 1993; 16:5276–5280. [PubMed: 8349568]
24. Arantes O, Lereclus D. Construction of cloning vectors for *Bacillus thuringiensis*. Gene. 1991; 108:115–119. [PubMed: 1662180]
25. Wu D, Johnson JJ, Federeci BA. Synergism of mosquitocidal toxicity between CytA and CryIV proteins using inclusions produced from cloned genes of *Bacillus thuringiensis* subsp. *israelensis*. Mol. Microbiol. 1994; 13:965–972. [PubMed: 7854129]
26. Muñóz-Garay C, Portugal L, Pardo-López L, Jiménez-Juárez N, Arenas I, Gómez I, Sánchez-López R, Arroyo R, Holzenburg A, Savva ChG, Soberón M, Bravo A. Characterization of the mechanism of action of the genetically modified Cry1AbMod toxin that is active against Cry1Ab-resistant insects. Biochim. Biophys. Acta Biomemb. 2009; 1788:2229–2237.
27. Thomas WE, Ellar DJ. *Bacillus thuringiensis* var. *israelensis* crystal delta-endotoxin: effects on insect and mammalian cells *in vitro* and *in vivo*. J. Cell Sci. 1983; 60:181–197. [PubMed: 6874728]
28. Schägger H, von Jagow G. Tricine-sodium dodecyl sulphate-polyacrylamide gel electrophoresis for the separation of proteins in the range from 1 to 100 kDa. Anal. Biochem. 1987; 166:368–379. [PubMed: 2449095]
29. Macek P, Sendicic L, Lebez D. Isolation and partial characterization of three lethal and hemolytic toxins from the sea anemone *Actinia cari*. Toxicon. 1982; 20:181–185. [PubMed: 6123161]
30. Finney, D. Probit analysis. Cambridge University Press; 1971. p. 50-80.
31. Rausell C, García-Robles I, Sánchez J, Muñoz-Garay C, Martínez-Ramírez AC, Real MD, Bravo A. Role of toxin activation on binding and pore formation activity of the *Bacillus thuringiensis* Cry3 toxins in membranes of *Leptinotarsa decemlineata* [Say]. Biochem. Biophys Acta. 2004; 1660:99–105. [PubMed: 14757225]
32. Chow E, Singh GJP, Gill SS. Binding and aggregation of the 25 kDa toxin of *Bacillus thuringiensis* subsp *israelensis* to cell membranes and alteration by monoclonal antibodies and amino acid modifiers. Appl. Environ. Microbiol. 1993; 55:2779–2788. [PubMed: 2624459]
33. Maceva SD, Puztai-Carey M, Russo PS, Butko P. A detergent-like mechanisms of action of the cytolytic toxin Cyt1A from *Bacillus thuringiensis* var. *israelensis*. Biochemistry. 2005; 44:589–597. [PubMed: 15641784]
34. Du J, Knowles BH, Li J, Ellar DJ. Biochemical characterization of *Bacillus thuringiensis* cytolytic toxins in association with phospholipid bilayer. Biochem. J. 1999; 338:185–193. [PubMed: 9931315]
35. Promdonkoy B, Ellar DJ. Investigation of the pore forming mechanism of cytolitic δ-endotoxin from *Bacillus thuringiensis*. Biochem. J. 2003; 374:255–259. [PubMed: 12795638]
36. Promdonkoy B, Rungrod A, Promdonkoy P, Pathaichindachote W, Krittanai Ch, Panyim S. Amino acid substitutions in αA and αC of Cyt2Aa2 alter hemolytic activity and mosquito-larvicidal specificity. J. Biotechnol. 2008; 133:287–293. [PubMed: 18054404]

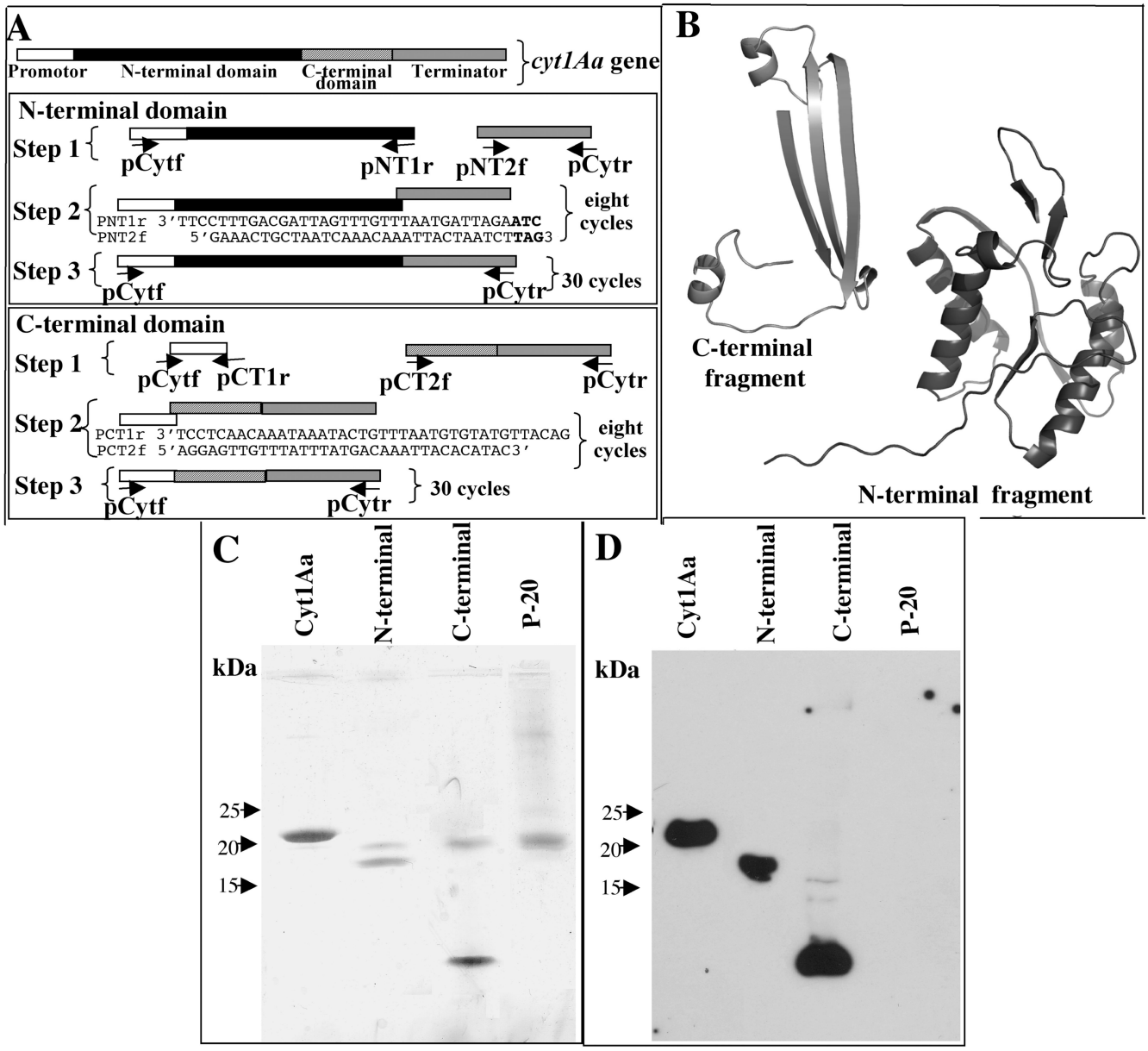

FIGURE 1. Cloning and expression of N- and C-terminal domains of Cyt1Aa toxin

Panel A, schematic representation of the *cyt1Aa* gene and the PCR procedure used to amplify and finally clone each one of the two protein fragments. Sequences of primers are shown in table 1. Panel B, putative three-dimensional structure of the two Cyt1Aa fragments according to the coordinates of Cyt2Aa. Panel C, silver stained SDS-PAGE von Javow gradient gel showing that N terminal fragment has a size of 18.9 kDa, and the C terminal fragment of 8.8 kDa. Panel D, Western blot analysis of N- and C-terminal fragments detected with polyclonal anti-Cyt1Aa1/11 antibody and a secondary Goat-HRP antibody. Size of proteins was estimated from molecular pre-stained precision plus standard, all blue (BioRad).

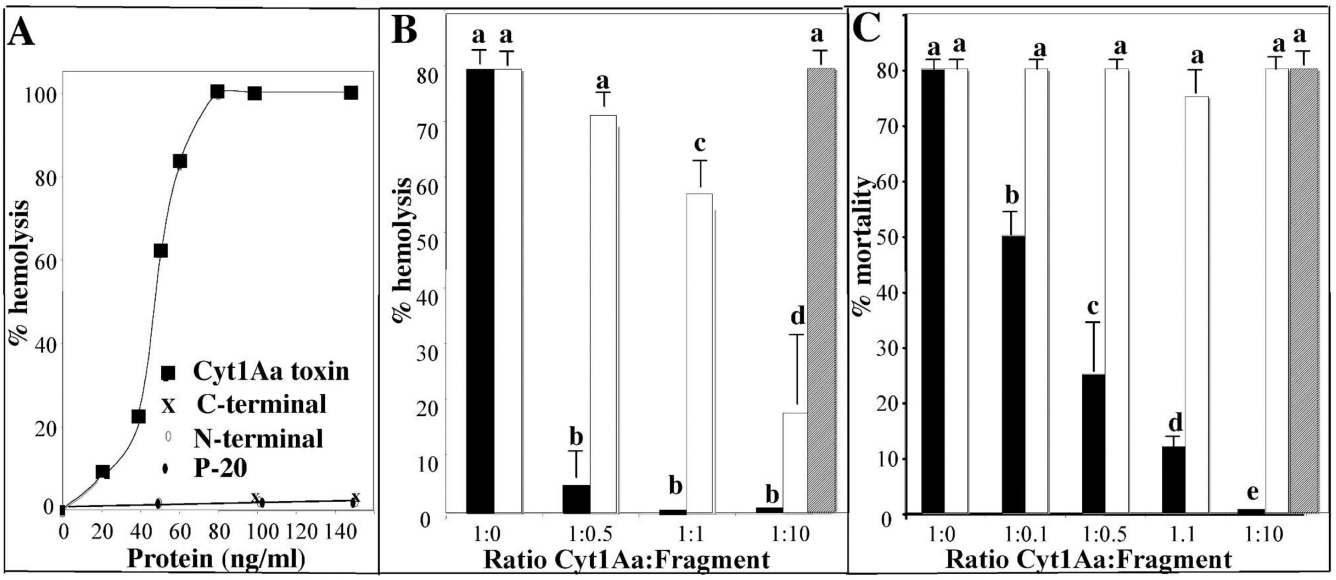

FIGURE 2. Effect of N- and C-terminal domains of Cyt1Aa toxin on hemolytic activity of Cyt1Aa in red blood cells and on *in vivo* insecticidal activity of Cyt1Aa against *Aedes aegypti* larvae

Panel A, analysis of hemolytic activity of activated Cyt1Aa protein or its N- and C-terminal domains against red blood cells as described in experimental procedures. ■, Cyt1Aa toxin; ◇, N-terminal domain; X, C-terminal domain; and ◆. P-20 protein. Panel B, analysis of the effect of N- and C- terminal fragments at different molar ratios on Cyt1Aa hemolytic activity. The fragments were pre-mixed with a Cyt1Aa protein concentration that gave 80 % hemolytic activity (60 ng/ml). Panel C, analysis of the effect of N- and C- terminal fragments at different molar ratios on Cyt1Aa insecticidal activity against *A. aegypti* larvae. The fragments were pre-mixed with a Cyt1Aa protein concentration that that kill 80 % of the larvae (1.2 μg/ml). Each value in panel B and C represents the mean ±SD of four independent experiments. A *t*-test was used to analyze statistical differences of mean values of percentage of hemolysis or percentage of mortality induced by the toxin:fragment mixtures compared with the control (only toxin 1:0 ratio). Bars labeled with different letters indicated that differences were statistically significant. Black bars, mixtures of Cyt1Aa with N-terminal fragment; white bars, mixtures of Cyt1Aa with C-terminal fragment and dashed bars represent the mixture of p20 protein with Cyt1Aa.

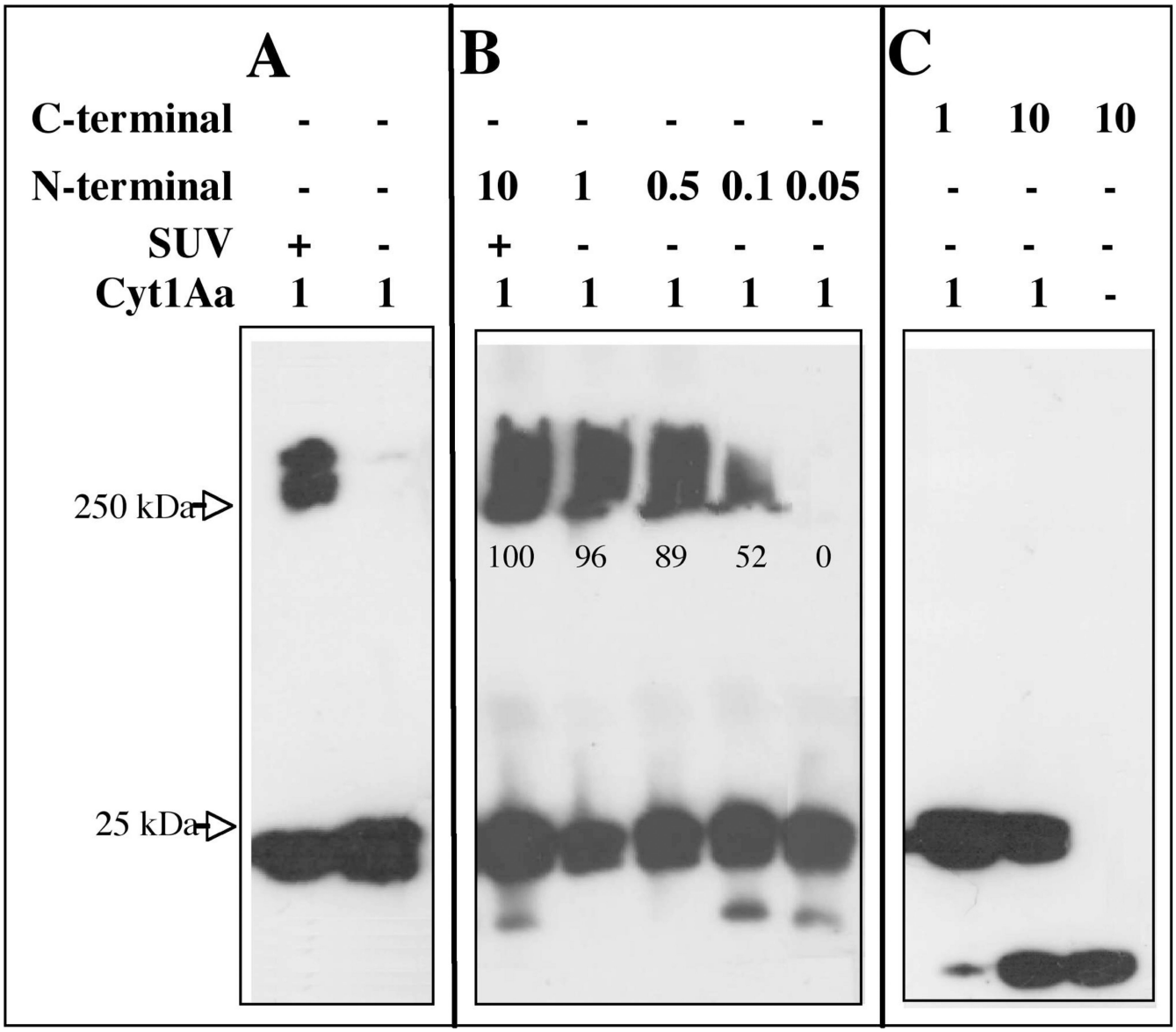

FIGURE 3. Analysis of Cyt1Aa oligomer formation by Western blot using polyclonal anti-Cyt1Aa/11 antibody and a secondary Goat-HRP antibody

Panel A, Cyt1Aa protoxin was activated with proteinase K in the presence or absence of SUV (PC:Ch:S mixture) liposomes. Panel B, analysis of the effect of N- terminal fragment at different molar ratios on oligomerization of Cyt1Aa in absence of lipid membranes. N-terminal fragment triggers aggregation of Cyt1Aa in absence of lipid membranes. Panel C, analysis of the effect of C- terminal fragment at different molar ratios on oligomerization of Cyt1Aa in absence of lipid membranes. Size of proteins was estimated from molecular pre-stained precision plus standard, all blue (BioRad). Numbers within the images represent the percentage of aggregate that was formed in the presence of N-terminal fragment as determine by scanning optical density of bands in the blots

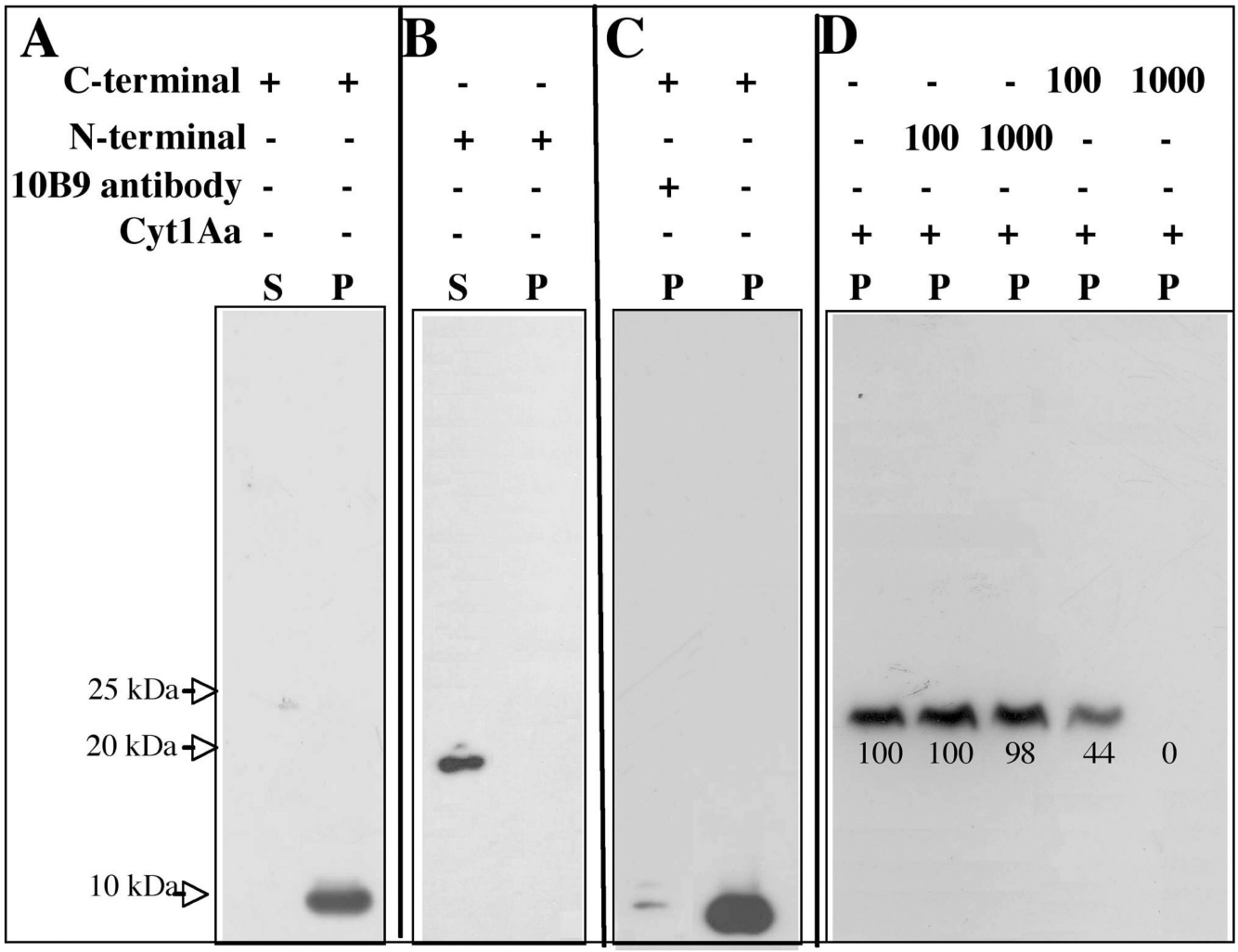

FIGURE 4. Analysis of interaction of N-terminal or C-terminal fragments with the membrane

Panel A, C-terminal fragment was incubated with SUV (PC:Ch:S mixture) then the membrane fraction was separated by centrifugation at 90,000 rpm for 30 min and visualized by Western blot using polyclonal anti-Cyt1Aa/11 antibody and a secondary Goat-HRP antibody. Panel B, interaction of N terminal fragment with SUV, conditions were identical to Panel A. Panel C, effect of monoclonal antibody 10B9 at 3:1 molar ratio (10B9:Cyt1Aa) on the binding of C-terminal fragment to SUV liposomes. The presence of C-terminal fragment bound to the membrane was visualized by Western blot as described for panel A. Panel D, binding competitions assay analyzing the binding of biotin-labeled Cyt1Aa toxin to SUV liposomes in the presence of 100 fold or 1000 fold molar excess of unlabeled C- or N-terminal fragments. The bioninylated toxin was visualized with streptavidin-HRP conjugate Scanning optical density of the 25 kDa bands in the blot was performed to quantify binding. Size of proteins was estimated from molecular pre-stained precision plus standard, all blue (BioRad). S, supernatant and P, membrane pellet.

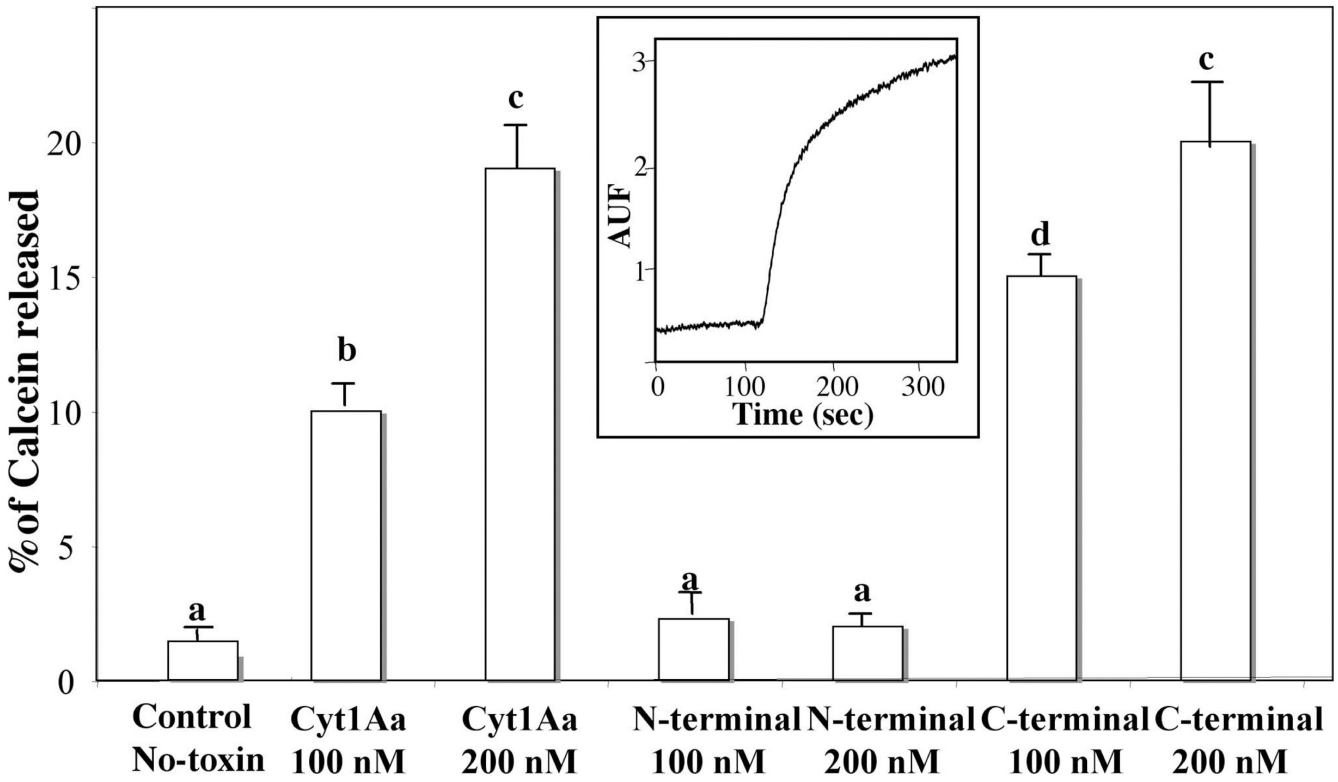

FIGURE 5. Analysis of pore formation activity of Cyt1Aa and its N-terminal and C-terminal fragments using calcein leakage assay

Calcein loaded SUV (PC:Ch:S mixture) suspended in 150 mM KCl, CHES 10 mM, pH 9, were incubated with the different protein samples at two concentrations and the release of calcein was analyzed. Maximal leakage at the end of each experiment was assessed with 0.1% Triton-X-100. Each value represents the mean ±SD of three independent experiments. A *t*-test was used to analyze statistical differences of mean values of percentage of calcein released by different concentrations of Cyt1Aa or the toxin-fragments when compared with the control (No-toxin). Bars labeled with different letters indicated that differences were statistically significant. Insert shows a representative trace of the calcein release assay performed with Cyt1Aa toxin.

TABLE 1

Sequence of primers used in PCR assays.

Primer name	sequence	Restriction site
p20f	5'AAA CCC GGG TTT GAC GAG GAA ACA GAG TAT ACG AGT T3'	*Xma*I
p20r	5'TTT CCC GGG AAA TCG AAC GTC ATA TAG ATA AAA TGC3'	*Xma*I
pCytf	5'ACA AAG CTT GGC ATC TTT CGA ACT ATA GC3'	*HindIII*
pCytr	5'GAT GGT ACC TAT GAA AAT ATA ACG TTG3'	*KpnI*
pNT1r	5'**CTA** AGA TTA GTA ATT TGT TTG ATT AGC AGT TTC CTT3'	none
pNT2f	5'GAA ACT GCT AAT CAA ACA AAT TAC TAA TCT **TAG**3'	none
pCT1r	5'GAC ATT GTA TGT GTA ATT TGT CAT AAA TAA ACA ACT CCT3'	none
pCT2f	5'AGG AGT TGT TTA TTT ATG ACA AAT TAC ACA TAC3'	none